Energy Systems Integration in Smart Districts: Robust Optimisation of Multi-Energy Flows in Integrated Electricity, Heat and Gas Networks

Eduardo Alejandro Martínez Ceseña, *Member, IEEE*, and Pierluigi Mancarella, *Senior Member, IEEE*

***Abstract*—Smart districts can provide flexibility from emerging distributed multi-energy technologies, thus bringing benefits to the district and the wider energy system. However, due to nonlinearity and modeling complexity, constraints associated with the internal energy network (e.g., electricity, heat, and gas) and operational uncertainties (for example, in energy demand) are often overlooked. For this purpose, a robust operational optimization framework for smart districts with multi-energy devices and integrated energy networks is proposed. The framework is based on two-stage iterative modeling that involves mixed integer linear programming (MILP) and linear approximations of the nonlinear network equations. In the MILP optimization stage, the time-ahead set points of all controllable devices (e.g., electrical and thermal storage) are optimized considering uncertainty and a linear approximation of the integrated electricity, heat, and gas networks. The accuracy of the linear model is then improved at a second stage by using a detailed nonlinear integrated network model, and through iterations between the models in the two stages. To efficiently model uncertainty and improve computational efficiency, multi-dimensional linked lists are also used. The proposed approach is illustrated with a real U.K. district; the results demonstrate the model's ability to capture network limits and uncertainty, which is critical to assess flexibility under stressed conditions.**

***Index Terms*—Multi-energy systems, MILP, integrated electricity heat and gas networks, robust optimisation, energy systems integration.**

NOMENCLATURE

Decision Variables (Optimisation)

C	Cost (£)
Ei, ***Eo***	Electricity input/output (kW_e)
Eoc	Electricity output curtailment (kW_e)
Gi	Gas inputs (kW_{th})
Hi, ***Ho***	Heat input/output (kW_{th})
I	Integer variable $\in [0, 1]$
L	Losses (kWh)
PF	Penalty function (£)
SOC	State of charge of storage unit (kWh)
xPF	Penalty for network constraint violations (£).

Network Simulation Parameters and Variables

B	Susceptance (S)
Cp	Heat capacity of water (4.182) (kJ/kg°C)
Dg, Dh	Pipe diameter (gas and heat) (mm^2)
$Fm2W$	Conversion factor from flow rate to power (Nh/m^2s)
G	Conductance (S)
$\dot{m}g$, $\dot{m}h$	Mass flow rates (gas and heat) (kg/s)
p	Pressure (gas) (bar)
Ts,Tr	Temperatures (supply and return) (°C)
V	Voltage magnitude (°)
θ	Voltage angle (°)
λ	Heat transfer coefficient (W/m°C)
ρg, ρh	Roughness of a pipe (m)
ℓg, ℓh	Pipe length (gas and heat) (m).

Parameters

ae, ah,	Linearization coefficients
Com	Cost - operation and maintenance (£)(£/kWh)
dt	Length of a time period (h)
ED	Electricity demand (kW_e)
$Emin$	Minimum electrical output (kW_e)
$Emax$	Maximum electrical output (kW_e)
$Esun$	Solar radiation (kW_e)
GD	Gas demand (kW_{th})
HD	Heat demand (kW_{th})
$Hmax$	Maximum thermal output (kW_{th})
Kf	Constant for network limits
Kfc	Independent parameter of linear constraint
Kfd	Dependent parameter of linear constraint
R	Ramp rate limits (kW)
$SOCmax$	Maximum state of charge (kWh)
$SOCmin$	Minimum state of charge (kWh)
ηe, ηh	Electrical/thermal efficiency (%)
πEi, πEo	Price of electricity imports/exports (outputs) ($£/kWh_e$)
πGi	Price of gas ($£/kWh_{th}$)

Manuscript received July 24, 2017; revised February 17, 2018; accepted March 27, 2018. Date of publication April 18, 2018; date of current version December 19, 2018. This work was supported by the U.K. EPSRC through the MY-STORE Project under Grant EP/N001974/1. Paper no. TSG-01035-2017. *(Corresponding author: Eduardo Alejandro Martínez Ceseña.)*

E. A. Martínez Ceseña is with the School of Electrical and Electronic Engineering, Electrical Energy and Power Systems Group, University of Manchester, Manchester M13 9PL, U.K. (e-mail: eduardo.martinezcesena@manchester.ac.uk).

P. Mancarella is with the Department of Electrical and Electronic Engineering, University of Melbourne, Melbourne, VIC 3010, Australia, and also with the School of Electrical and Electronic Engineering, University of Manchester, Manchester M13 9PL, U.K. (e-mail: p.mancarella@manchester.ac.uk).

Color versions of one or more of the figures in this paper are available online at http://ieeexplore.ieee.org.

Digital Object Identifier 10.1109/TSG.2018.2828146

ω_s Probability of occurrence of scenario/period s (%).

Sets

BEN	Buildings connected to an electricity network
BGN	Buildings connected to a gas network
BHN	Buildings connected to a heat network
RCHD	Robust constraints (heat demand)
RCED	Robust constraints (electricity demand0
RCPV	Robust constraints (solar radiation).

Superscripts

Blr	Boiler
Bui	Building
CHP	Combined Heat and Power
Dis	District
EHP	Electric Heat Pump
EES	Electrical Energy Storage
PV	Photovoltaic system
TES	Thermal Energy Storage
Net	Network.

Indices

b	Buildings
i, j	Nodes (electricity, heat and gas)
ne, nh, ng	Electricity, heat and gas networks
s	Time periods (associated with a scenario).

I. Introduction

SMART districts are emerging as a means to exploit flexibility from the coordinated operation of multi-energy technologies that are being integrated at the building and district levels [1]. To name a few, these technologies include Electric Heat Pumps (EHP), Combined Heat and Power (CHP) plants, gas boilers, Electrical Energy Storage (EES), Thermal Energy Storage (TES), solar Photovoltaic (PV) systems, and so forth. By optimally coordinating the set points of these devices (e.g., the equivalent of a day-ahead Unit Commitment - UC), smart districts aim to provide a wide range of benefits including costs and emissions savings for the district, and provision of energy, reserve and other services to the wider energy system [2]. However, properly modelling and quantifying these benefits, and understanding the flexibility of smart multi-energy districts is a daunting task that involves complex impacts on different networks (e.g., electricity, heat and gas) and spatial, temporal, and multi-vector interactions in response to uncertain energy demand [3], amongst others. Due to this complexity, the operation of the district is generally optimised with little or no regard for the internal networks and relevant constraints, which could lead to infeasible results (i.e., exceeding network limits).

The complexity of smart multi-energy districts lies on their flexibility to exploit different energy vectors (e.g., electricity heat and gas). This is achieved through managing the set points of CHP, EHP, storage and other distributed technologies (located in different buildings), which effectively couple the electricity distribution, district heating, gas and other networks within the district [4]. The impacts of the now integrated network become more critical due to costly network upgrades that would be required for the increasing adoption of distributed technologies [1]. It would be significantly more economically attractive to use part of the flexibility of the smart district to actively manage the integrated network.

In order to properly model realistic operation of smart multi-energy districts, including impacts on the integrated network, available optimisation and simulation tools must be improved [3]. Existing optimisation tools can model district operation in light of uncertainty, inter-temporal constraints (e.g., associated with storage) and different economic considerations [5]–[7]. Yet, these tools tend to simplify the district by aggregating devices at the building or district levels (e.g., using the energy hub approach [3]). In addition, the tools either neglect the integrated network, or rely on simplified approximations of the network equations [8]. As a result these studies may provide infeasible solutions that may violate the technical limits of the integrated networks, especially if the networks are not constantly upgraded as discussed above.

Existing simulation models generally avoid infeasible network conditions by providing accurate representations of network parameters (e.g., losses) and stress conditions associated with thermal, pressure, voltage and other technical limits [4], [9]. Furthermore, some of these models have been extended to include optimisation of multi-energy technologies within an Optimal Power Flow (OPF) framework [9]. Nevertheless, these tools still rely on simplifications (e.g., snapshots, predefined use of storage, etc.) which do not properly capture the combined complexity of multi-flow interactions, uncertainty and inter-temporal constraints.

Based on the above, this paper aims to shed light on the feasibility and economic value of smart districts by considering realistic conditions where the operation of a wide range of multi-energy technologies (including storage) must be optimised considering uncertainty and limitations of the integrated electricity, heat and gas network. For this purpose a new Mixed Integer Linear Programming (MILP) framework is proposed for the robust optimisation of smart multi-energy districts in light of uncertainty, different devices (e.g., PV, EHP, CHP, EES, TES and gas boilers) and detailed integrated electricity, heat and gas network models. The MILP formulation is used to optimise the time-ahead operation (set points) of all technologies within a district. Uncertainty is modelled with scenarios for solar radiation and electricity and heat demand. Robust constraints and multi-stage techniques are used to identify operation schedules that are both robust to external changes, and which can be adjusted in light of pre-specified scenarios. The detailed characteristics of the integrated network are addressed using a two-stage approach. That is, the MILP model is first solved without consideration of the networks. Afterwards, a detailed integrated model is used to assess the networks' operational state and produce linear approximations of losses and constraint violations. The two-stage process is repeated until achieving the desired level of accuracy. An additional feature of the proposed approach is the formulation of

the MILP problem using linked lists to improve computational efficiency [10].

The proposed framework is demonstrated with a real multi-energy district in the U.K. Different cases for penetration of smart technologies, uncertainty levels, and network constraints are presented to highlight the features of the algorithms, as well as the importance of modelling uncertainty, time-dependence and network limits. Accordingly, the main contributions of this paper are as follows:

(i) New iterative two-stage framework that captures the flexibility inherent in smart multi-energy districts considering the physical characteristics of the underlying integrated electricity, heat and gas network.

(ii) New robust optimisation MILP framework that explicitly captures complexity from uncertainty, and inter-temporal constraints (e.g., associated with storage).

(iii) Use of multi-dimensional linked lists to efficiently model non-anticipativity constraints and improve computational efficiency.

(iv) Pragmatic case study based on a real multi-energy district, which demonstrates and quantifies the impacts of uncertainty, time-dependency and network limits.

The rest of the paper is structured as follows. Section II presents a relevant literature survey. The proposed two-stage approach is then described in Section III and illustrated with a real multi-energy district in Section IV. The main findings and conclusions are summarised in Section V.

II. Literature Survey

The potential of smart multi-energy districts to reduce energy costs and support the energy system is widely recognised [1], [11]. However, due to the underlying complexity, existing literature tends to focus on the operation of smart districts (e.g., considering time dependences, uncertainty, and so forth) without detailed consideration of the underlying integrated network. Alternatively, detailed studies of integrated networks, including active network management, tend to be based on simplified district operation models.

The underlying complexity of smart multi-energy districts has motivated the use of simplifications, especially by aggregating multi-energy technologies at the buildings or districts levels [3]. This aggregation is typically achieved by formulating energy hubs, which provide input and output interfaces that couple all multi-energy technologies within buildings, districts, etc. [5]. The simplified representation of smart districts as energy hubs, facilitates researching flexibility from complex multi-vector interactions between the district and the energy system, time dependences (e.g., from storage) and uncertainty within an optimisation framework [3]. For example, the aggregated flexibility of the district (or building) can be used to minimise district costs and emission and provide multiple services to the wider energy system [2], [12]. In this context, multi-energy storage is critical for facilitating time arbitrage (e.g., importing energy when prices are low) and mitigating impacts of uncertain demand, generation, system needs and so forth [6], [7].

These findings have directed attention to the importance of properly modelling uncertainty, e.g., using robust constraint and multi-stage approaches [13], [14]. Whilst robust constraints do not fully capture district flexibility to respond to combinations of uncertain scenarios [6], the constraints ensure that the system can cope with worst case conditions [15]. Furthermore, the models tend to be computationally tractable, and can be coupled with policies or algorithms (e.g., dynamic programming) that define the use of storage [16], [17]. Conversely, multi-stage approaches provide reasonably accurate representation of uncertainty and flexibility, including flexibility from storage [14]. However, these methods can become computationally costly or infeasible, as the required number of variables increases exponentially with the number of stages under consideration. This issue can be mitigated by constraining the use of variables, e.g., by clustering similar scenarios into buckets, which can then be used to limit the size of the scenario trees required for multi-stage approaches [6].

The aggregated (energy hub) district representation has facilitated novel research on optimised district flexibility. However, this approach has the disadvantages of making the district difficult to customise and oversimplifying critical system parameters [3], [18]. Some parameters such as inputs or outputs of groups of similar technologies (e.g., all CHPs in the district) can still be accessed using energy hub layering [19], yet connection points to the integrated network are still concealed. This is an issue for analysing network stress within the district, and deploying flexibility for active network management [20]. These aspects must be considered to guarantee that the optimised operation of the district is feasible (i.e., network limits are met).

Properly modelling the integrated network is critical for assessing the value of smart districts. This is because, due to economic reasons, network stress levels are likely to raise with the adoption of multi-energy technologies (i.e., reinforcement costs can become significant). However, properly modelling the integrated network (e.g., electricity, heat and gas) is, by itself, a current research challenge. Available multi-energy literature offers options to optimise districts considering simplified representations of the integrated network [8]. Yet, detailed network modelling is usually reserved for external networks (after aggregating the district) [11], [21], or applications based on simplified district operation models that, for example, neglect uncertainty, only address two networks, analyse single snapshots, etc. [22]–[24]. In fact, dedicated integrated network simulation methods (without district optimisation capabilities), are still being researched and developed [3]. Energy hubs are, once again, popular tools for the analysis of multiple or integrated network models. This time, rather than aggregating multi-energy technologies, the hubs are applied per device to either soft-link different network models that can be solved independently [3], [8], or actively link the networks to develop detailed, integrated network simulation models [4], [25].

It is clear that a tool that can properly optimise district operation and model the integrated network is critical for understanding the feasibility and value of smart multi-energy district. Accordingly, this paper proposes an integrated framework that can address both aspects, specifically optimal coordination

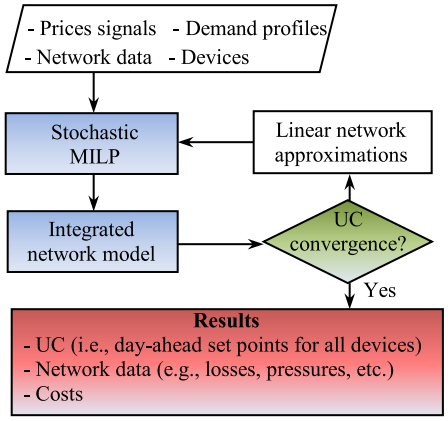

Fig. 1. High level flow diagram of multi-energy district optimisation.

of multi-energy flows per device, uncertainty, inter-temporal constraints (e.g., from BES and TES), and impacts on, including active management of, the integrated electricity, heat and gas network. The framework does not include all these considerations in a single mathematical model, as this may be computationally challenging or infeasible [26], [27]. Instead, the proposed integrated framework is built by decoupling optimisation and network simulation engines, and iteratively exchanging information between the two modules using a two-stage process. The complexity of each model is also reduced through multi-dimensional linked lists formulation. Further details about the integrated framework are provided below.

III. Methodology

In this section a new integrated framework that identifies the optimal time-ahead set points (e.g., day-ahead UC) for all controllable devices within a smart multi-energy district is presented. The two-stage framework combines a stochastic MILP and a detailed integrated electricity, heat and gas model. A high level representation of the approach is shown in Fig. 1.

The optimisation model formulates a first estimation of the UC based on available price signals, energy demand profiles and characteristics of devices (networks are ignored at this stage). This information is then passed to the network model, which estimates losses and identifies existing network constraint violations (if any). This information is used to formulate piece-wise linear estimations of losses and network constraints that are passed back to the optimisation model. The two-stage process is then iteratively repeated until the results converge to a point where losses remain unchanged and network violations are averted (or cannot be further alleviated). More details about the optimisation and network models (including a section dedicated to uncertainty modelling), and the two-stage approach are provided below.

It is important to note that, for the sake of simplicity, the nomenclature provided above relies on a simplified superscript based representation of the large number of variables and parameters used by the model. That is, for example, the variable for electricity outputs ($\boldsymbol{Eo}$) is combined with different superscripts to denote different variables such as electricity outputs from a solar system ($\boldsymbol{Eo^{PV}}$), CHP device ($\boldsymbol{Eo^{CHP}}$), building ($\boldsymbol{Eo^{Bui}}$), point of connection of a network ($\boldsymbol{Eo^{Net}}$), the whole district ($\boldsymbol{Eo^{Dis}}$), etc. All variables are indicated in bold for clarity.

A. Optimisation Model

The proposed optimisation engine is built on a flexible MILP formulation proposed in [28]. This formulation is extended here to include energy storage (i.e., EES and TES), additional inter-temporal constraints (e.g., ramp constraints) and operational uncertainty.

The objective of the optimisation, denoted by (1), is the minimisation of expected time-ahead energy costs. This is based on (i) the electricity imported and exported by the whole district at the point of connection, as internal electricity flows between customers are not charged; (ii) gas imported by the district, (iii) operation and maintenance costs for CHP, EHP, PV, boilers, and storage devices, which is a function of their operation; and (iv) a penalty function for infeasible and undesired conditions, e.g., network violations and curtailment.

$$\begin{aligned} &\textit{Minimise}: \\ &\boldsymbol{C} = dt \times \sum_{s} \omega_s \times \Big[\pi Ei_s \times \boldsymbol{Ei}_s^{Dis} - \pi Eo_s \times \boldsymbol{Eo}_s^{Dis} + \pi Gi_s \\ &\qquad \times \boldsymbol{Gi}_s^{Dis} + \sum_{b} \Big(\boldsymbol{Eo}_{b,s}^{CHP} \times Com_b^{CHP} \\ &\qquad + \boldsymbol{Ho}_{b,s}^{EHP} \times Com_b^{EHP} + Com_b^{PV} + \boldsymbol{Ho}_{b,s}^{Blr} \\ &\qquad \times Com_b^{B} + Com_b^{EES} + Com_b^{TES}\Big)\Big] + \boldsymbol{PF} \end{aligned} \tag{1}$$

The heat output of the gas boilers, which is a function of the gas imports and efficiency as denoted by (2), must be within limits as modelled with (3).

$$\boldsymbol{Ho}_{b,s}^{Blr} = \eta h_b^{Blr} \times \boldsymbol{Gi}_{b,s}^{Blr} \qquad \forall_{b,s} \tag{2}$$

$$0 \le \boldsymbol{Ho}_{b,s}^{Blr} \le Hmax_b^{Blr} \qquad \forall_{b,s} \tag{3}$$

The electricity and thermal outputs of CHP devices are respectively represented with (4) and (5) as linear functions of the gas input and by using a binary variable and two parameters. As discussed in [28], these linear equations can represent typical nonlinear electrical and thermal efficiency functions given by manufacturers (alternative approaches can be found in [29]). Generation limits are imposed with (6) and ramp constraints (time dependent equations) are modelled with (7). The binary variables are used to switch the devices on or off.

$$\boldsymbol{Eo}_{b,s}^{CHP} = \boldsymbol{I}_{b,s}^{CHP} \times ae1_b^{CHP} + \boldsymbol{Gi}_{b,s}^{CHP} \times ae2_b^{CHP} \qquad \forall_{b,s} \tag{4}$$

$$\boldsymbol{Ho}_{b,s}^{CHP} = \boldsymbol{I}_{b,s}^{CHP} \times ah1_b^{CHP} + \boldsymbol{Gi}_{b,s}^{CHP} \times ah2_b^{CHP} \qquad \forall_{b,s} \tag{5}$$

$$-R_b^{CHP} \times dt \le \boldsymbol{Eo}_{b,s}^{CHP} - \boldsymbol{Eo}_{b,s-1}^{CHP} \le R_b^{CHP} \times dt \qquad \forall_{b,s} \tag{6}$$

$$\boldsymbol{I}_{b,s}^{CHP} \times Emin_b^{CHP} \le \boldsymbol{Eo}_{b,t}^{CHP} \le \boldsymbol{I}_{b,s}^{CHP} \times Emax_b^{CHP} \qquad \forall_{b,s} \tag{7}$$

The heat output, generation capacity and ramp constraints used to model EHPs are (8), (9) and (10), respectively. As in the case of CHP devices, the ramp constraints capture time dependencies.

$$\boldsymbol{Ho}_{b,s}^{EHP} = \boldsymbol{Ei}_{b,s}^{EHP} \times \eta h_b^{EHP} \qquad \forall_{b,s} \tag{8}$$

$$0 \le \boldsymbol{Ho}_{b,s}^{EHP} \le Hmax_b^{EHP} \qquad \forall_{b,s} \tag{9}$$

$$-R_b^{EHP} \times dt \leq \boldsymbol{Ho}_{b,s}^{EHP} - \boldsymbol{Ho}_{b,s-1}^{EHP} \leq R_b^{EHP} \times dt \quad \forall_{b,s} \quad (10)$$

PV generation is modelled based on the solar resource and the option to curtail energy outputs, as denoted by (11).

$$\boldsymbol{Eo}_{b,s}^{PV} = dt \times \eta e_b^{PV} \times Esun_s^{PV} - \boldsymbol{Eoc}_s^{PV} \quad \forall_{b,s} \quad (11)$$

The time dependent energy outputs and inputs and SOC of the EES and TES are respectively modelled with (12) and (13). Limits on the energy that can be stored in the devices, in terms of the SOC, are modelled with (14) and (15). Ramp constraints on the rate of charge and discharge of the devices are denoted by (16) and (17). Additional constraints to avoid simultaneous charging and discharging could also be considered. However, those constraints were not added, as such conditions do not arise in this particular model due to economic reasons (see energy balance below).

$$\boldsymbol{Eo}_{b,s}^{EES} - \boldsymbol{Ei}_{b,s}^{EES} = dt \times \left(\boldsymbol{SOC}_{b,s}^{EES} - \boldsymbol{SOC}_{b,s-1}^{EES}\right) \quad \forall_{b,s} \quad (12)$$

$$\boldsymbol{Ho}_{b,s}^{TES} - \boldsymbol{Hi}_{b,s}^{TES} = dt \times \left(\boldsymbol{SOC}_{b,s}^{TES} - \boldsymbol{SOC}_{b,s-1}^{TES}\right) \quad \forall_{b,s} \quad (13)$$

$$SOCmax^{EES} \geq \boldsymbol{SOC}_{b,s}^{EES} \geq SOCmin^{EES} \quad \forall_{b,s} \quad (14)$$

$$SOCmax_b^{TES} \geq \boldsymbol{SOC}_{b,s}^{TES} \geq SOCmin_b^{TES} \quad \forall_{b,s} \quad (15)$$

$$-R_b^{EES} \times dt \leq \boldsymbol{SOC}_{b,s}^{EES} - \boldsymbol{SOC}_{b,s-1}^{EES} \leq R_b^{EES} \times dt \quad \forall_{b,s} \quad (16)$$

$$-R_b^{TES} \times dt \leq \boldsymbol{SOC}_{b,s}^{TES} - \boldsymbol{SOC}_{b,s-1}^{TES} \leq R_b^{TES} \times dt \quad \forall_{b,s} \quad (17)$$

Alternative formulations may include consideration of the impacts of temperature, which may be particularly relevant for TES modelling if the characteristics of the building and thermal comfort preferences are also defined [7]. Regarding BES, the ramp constraints (16) and (17) could be replaced with nonlinear models of SOC variations associated with rapid battery charge or discharge rates (e.g., beyond the ramp constraints). Piece-wise linear approximations of the constraints could be considered at the expense of increasing computational complexity. However, operating the batteries in this manner can cause degradation over the years [30], which would be better addressed from an investment perspective [31], [32]. As the focus of this work is on operation and investments are not addressed, nonlinear SOC variations and degradation are not considered.

Energy balance is modelled at the building, network and district levels. At the building level, all generation surplus or deficit is balanced by the network as denoted by (18), (19) and (20). It is worth noting that, given the technologies considered in this work, gas exports to the network are not included.

$$\begin{aligned} ED_{b,s}^{Bui} &= \boldsymbol{Eo}_{b,s}^{Bui} - \boldsymbol{Ei}_{b,s}^{Bui} + \boldsymbol{Eo}_{b,s}^{CHP} + Eo_{b,s}^{PV} - \boldsymbol{Eo}_{b,s}^{EHP} \quad \forall_{b,s} \\ &\quad + \eta e1_b^{TES} \times \boldsymbol{Eo}_{b,s}^{EES} - \eta h2_b^{EES} \times \boldsymbol{Ei}_{b,s}^{EES} \end{aligned} \quad (18)$$

$$\begin{aligned} HD_{b,s}^{Bui} &= \boldsymbol{Ho}_{b,s}^{Bui} - \boldsymbol{Hi}_{b,s}^{Bui} + \boldsymbol{Ho}_{b,s}^{B} + \boldsymbol{Ho}_{b,s}^{CHP} + \boldsymbol{Ho}_{b,s}^{EHP} \\ &\quad + \eta h1_b^{TES} \times \boldsymbol{Ho}_{b,s}^{TES} - \eta h2_b^{TES} \times \boldsymbol{Hi}_{b,s}^{TES} \quad \forall_{b,s} \end{aligned} \quad (19)$$

$$\boldsymbol{Gi}_s^{Bui} = \left(GD_{b,s} + \boldsymbol{Gi}_{b,s}^{Blr} + \boldsymbol{Gi}_{b,s}^{CHP}\right) \quad \forall_s \quad (20)$$

Considering that a district can comprise several networks, energy (including losses) is also balanced at the network level, e.g., at the point of connection or substation. Different electricity and heat networks, or network conditions (e.g., for N-1 security analysis) within the district, are modelled with (21) and (22). The gas network is not included at this stage as only a single gas network with a fixed configuration is considered in this work.

$$\begin{aligned} \boldsymbol{Ei}_{ne,s}^{Net} &= \boldsymbol{Eo}_{ne,s}^{Net} + \sum_{b \in BEN(ne)} \left(\boldsymbol{Ei}_{b,s}^{Bui} - \boldsymbol{Eo}_{b,s}^{Bui}\right) \\ &\quad + \boldsymbol{L}_{ne,s}^{Net} \quad \forall_{ne,s} \end{aligned} \quad (21)$$

$$\boldsymbol{L}_{nh,s}^{Net} = \sum_{b \in BHN(nh)} \left(\boldsymbol{Ho}_{b,s}^{Bui} - \boldsymbol{Hi}_{b,s}^{Bui}\right) \quad \forall_{nh,s} \quad (22)$$

At the district level, the net energy of the different networks is balanced by the upstream energy system. Only the equations for electricity (23) and gas (24) balancing are considered, as heat is locally balanced at the network level with centralised heat generation (e.g., gas boilers).

$$\boldsymbol{Ei}_s^{Dis} - \boldsymbol{Eo}_s^{Dis} = \sum_{ne} \left(\boldsymbol{Ei}_{ne,s}^{Net} - \boldsymbol{Eo}_{ne,s}^{Net}\right) \quad \forall_s \quad (23)$$

$$\boldsymbol{Gi}_s^{Dis} = \sum_{ng} \boldsymbol{L}_{ng,s}^{Net} + \sum_{b \in BGN(ng)} \boldsymbol{Gi}_s^{Bui} \quad \forall_s. \quad (24)$$

B. Modelling Robustness and Flexibility

In order to identify solutions that are both robust and flexible in the face of uncertainty, the proposed model includes N-1 security considerations for the electricity network, robust constraints and multi-stage trees.

N-1 security considerations are modelled with dedicated scenarios and (19) is in line with current U.K. security considerations (i.e., P2/6 engineering standards [33]) for medium voltage (6.6 kV and 11 kV) distribution networks. Robust constraints are modelled using predefined sets of worst case conditions for electricity (25) and heat demand (26), and solar generation (27). These scenarios can be formulated offline using a wide range or approaches and desired degree of robustness [14], [34]. Dedicated scenarios with specific sets of decision variables and consideration of intertemporal constraints are used to model the robust constraints. Note that the intertemporal constraints include ramp constraints and weighted sums to link the SOC of the different storage devices to a centralised (average) scenario.

$$ED_{b,s}^{Bui} \in RCED(b,s) \quad \forall_{b,s} \quad (25)$$

$$HD_{b,s}^{Bui} \in RCHD(b,s) \quad \forall_{b,s} \quad (26)$$

$$Esun_s^{PV} \in RCHD(s) \quad \forall_{b,s} \quad (27)$$

The robust formulation defined above can over or under estimate the use (and flexibility) of storage as, in practice, the operation of the district will deviate from expected average conditions. This issue could be solved with multi-stage formulation which allows considering different SOCs, but such approach would be computationally expensive [14]. However, as discussed in [6], computational costs can be minimised when modelling flexible operation of storage by constraining scenarios within buckets (based on their similarities). Following this philosophy, sets of scenario trees spanning from the average scenario for a couple of periods (two in this work) are added to the model. These constraints will be hereinafter referred to as *flexibility constraints*.

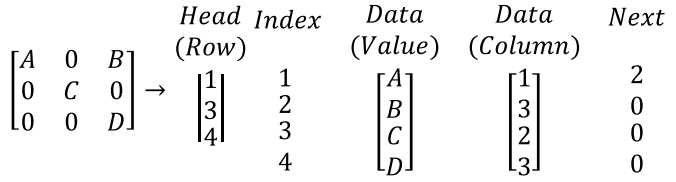

Fig. 2. Data stored in an array and the equivalent linked list.

It is important to highlight that the proposed framework does not include the typical non-anticipativity constraints that would be required for the formulation of security, robust and flexibility constraints. Instead, and also with the aim of improving computational efficiency, the proposed framework is formulated using multi-dimensional linked lists [10]. To illustrate this, note that the equations presented throughout this paper are based on a matrix representation of data (e.g., $\boldsymbol{Eo}_{b,s}^{CHP}$ can be seen as a variable in row b, column s). These matrices may be sparse (e.g., some buildings may not have CHPs or other devices) or contain redundant variables (e.g., non-anticipativity constraints can be introduced by connecting redundant variables). Alternatively, these matrices can be represented as a series of linked lists (see Fig. 2). These lists include a *Head* that provides the location (*Index*) of specific data types, such as particular devices, constraints, scenarios, etc. The specified location provides information for a single element (e.g., capacity, time period, scenario and so forth), and the location of the *Next* element. A null value (zero in the example) is provided to indicate that there are no further parameters matching the requested data type.

Based on the linked list formulation, specific devices and scenarios (including trees with different shapes) can be seamlessly included or removed from the mathematical model. For example, by adjusting the *Next* list, specified devices are skipped in the heat balance equations (18), and non-anticipativity constraints are created. This additional feature of the proposed method allows minimisation of variables and significantly improves computational efficiency.

C. Integrated Network Model

The model used for steady-state modelling of the integrated electricity, heat and gas network is based on the tool proposed in [4]. However, here the tool has been further extended to account for loops in the heat and gas networks [9], [35].

The integrated network model is formulated by using efficiency matrices representing available multi energy technologies (e.g., EHP, CHP, etc.) as a means to couple the steady-state models of the electricity, heat and gas networks. The model is solved with the Newton method, which includes coupling elements in the Jacobian matrix if the networks are integrated [9]. The coupling elements are introduced by multi-energy technologies used as slack generators, or to provide active network management (e.g., pumps that control nodal pressures). Thus, if no coupling elements arise, the networks are decoupled and can be solved accordingly. Otherwise, the integrated network model is used.

The electricity network is modelled with typical power flow equations for active (28) and reactive (29) nodal balance.

$$\sum_{b\in BEN(ne,i)} active\left(\boldsymbol{Ei}_{b,s}^{Bui} - \boldsymbol{Eo}_{b,s}^{Bui}\right) = \forall_{ne,s}$$
$$\sum_{j} V_{i,s} \times V_{j,s} \times \begin{bmatrix} G_{i,j,s} \times cos\left(\theta_{i,s} - \theta_{j,s}\right) + \\ B_{i,j,s} \times sin\left(\theta_{i,s} - \theta_{j,s}\right) \end{bmatrix} \quad (28)$$

$$\sum_{b\in BEN(ne,i)} reactive\left(\boldsymbol{Ei}_{b,s}^{Bui} - \boldsymbol{Eo}_{b,s}^{Bui}\right) = \forall_{ne,s}$$
$$\sum_{j} V_{i,s} \times V_{j,s} \begin{bmatrix} G_{i,j,s} \times sin\left(\theta_{i,s} - \theta_{j,s}\right) - \\ B_{i,j,s} \times cos\left(\theta_{i,s} - \theta_{j,s}\right) \end{bmatrix} \quad (29)$$

The heat network is modelled based on nodal balance (30) and cumulative head losses (for looped networks) (31).

$$\sum_{b\in BHN(nh,i)} \left(\boldsymbol{Hi}_{b,s}^{Bui} - \boldsymbol{Ho}_{b,s}^{Bui}\right) = \sum_{j} Cp \times \dot{m}h_{i,j,s} \times \left(Ts_{i,s} - Tr_{i,s}\right) \quad \forall_{nh,s} \quad (30)$$

$$0 = \sum_{i}\sum_{j} \frac{\ell h_{i,j} \times \chi_{i,j} \times sign\left(\dot{m}h_{i,j,s}\right) \times \left(\dot{m}h_{i,j,s}\right)^2}{0.125 \times \rho h_{i,j}^2 \times \pi \times g \times \left(Dh_{i,j}\right)^2} \forall_{i,j} \quad (31)$$

The gas network is modelled based on nodal balance (32), pressure drops (33), and head losses (31).

$$\sum_{b\in BGN(ng,i)} \boldsymbol{Gi}_{b,s}^{Bui} = Fm2W \times \sum_{j} \dot{m}g_{i,j,s} \quad \forall_{ng,s} \quad (32)$$

$$p_{i,s} - p_{j,s} = \frac{\rho g_{i,j} \times \ell g_{i,j} \times \dot{m}g_{i,j,s} \times \left|\dot{m}g_{i,j,s}\right|}{Dg_{i,j}} \quad \forall_{i,j,s} \quad (33)$$

The Newton approach is used to iteratively calculate voltages and angles, mass flow rates, pressures and temperatures. Further details, and the full list of equations can be found in [9] and [35].

D. Iterative Two-Stage Approach

As discussed above, the proposed two-stage approach is based on the iterative formulation of piece-wise linear estimations of losses and network limits. The linear constraints are formulated by, firstly, estimating the operation of the district with the optimisation model, and estimating losses and network limits (e.g., capacity, voltage and pressure limits) with the integrated network model. Afterwards, the energy losses and (active) network constraints are differentiated with respect to electricity, heat and gas flows at the building level. Note that, if heat within a building is produced at different temperatures (e.g., the output temperatures of CHP and gas boilers are different), losses and constraints will have to be differentiated with respect to each heating technology. As denoted by (34), the differentials (*Kfd*) and an independent constant (*Kfc*) are then used to create linear approximations of the current constraint violations (and losses as estimated by the optimisation). This equation only represents a single constraint, also assuming that all devices produce heat at the same temperature. Additional constraints are introduced to create the piece-wise

approximation, and the penalty variable (***xPF***) is not included when modelling losses.

$$\begin{aligned} Kf_s \geq\ & Kfc_s - \boldsymbol{xPF}_s \\ & + \sum_i \sum_{b \in BEN(ne,i)} \left[Kfd_{ne,b,s} \times \left(\boldsymbol{Ei}^{Bui}_{b,s} - \boldsymbol{Eo}^{Bui}_{b,s} \right) \right] \\ & + \sum_i \sum_{b \in BHN(nh,i)} \left[Kfd_{nh,b,s} \times \left(\boldsymbol{Ei}^{Bui}_{b,s} - \boldsymbol{Eo}^{Bui}_{b,s} \right) \right] \\ & + \sum_i \sum_{b \in BGN(ng,i)} \left[Kfd_{ng,b,s} \times \left(\boldsymbol{Gi}^{Bui}_{b,s} - \boldsymbol{Eo}^{Bui}_{b,s} \right) \right] \end{aligned} \quad (34)$$

These constraints would not force the optimiser to update the UC, as the current solution would still be feasible, and losses would be the same. Thus, before the next iteration, the independent parameters (Kfc_s) must be adjusted to push the solution closer to the simulated conditions. However, this is not a trivial task as large adjustments per iteration may turn the optimisation problem infeasible. Therefore, a suitable methodology needs to be devised, as discussed below.

Existing OPF literature provides several approaches to integrate optimisation and electricity network modelling [13], [26], [27], which could be used to adjust both independent (Kfc_s) and dependent (Kfd) parameters. However, the optimality and convergence of those approaches has generally only been validated for specific electricity network conditions (e.g., without reverse power flows, for radial configurations, etc.) and definitely not in an integrated network context. Accordingly, a general secant method is used in this work. More specifically, the following steps are used:

1) Convergence criteria for the algorithm are defined. Based on OPF and UC literature [13], [26], [27], the criteria selected in this work includes (i) more accurate estimation of losses, (ii) reduced magnitude of constraint violations, and (iii) introduction of new constraint violations only if their highest value is lower than the average constraint reduction.

2) Baseline conditions are defined based on the network constraint violations and losses. The independent parameters (e.g., Kfc) are adjusted so that the linear constraints match the results of the integrated network simulation. The linear constraints are included in the next optimisation.

3) If the new UC meets all convergence criteria and, thus, the results of the model are converging, the previous step is repeated. Otherwise, new values for the independent parameters are estimated using linear interpolations between the baseline and the new data. The new sets of constraints are added to the optimisation, and this step is repeated. Alternatively, the process would meet the termination criterion if the UC has remained unchanged subject to a threshold for accuracy. The accuracy is measured as the maximum difference between the parameters used for the linear network approximations (e.g., Kfd and Kfc) in two consecutive iterations.

4) The UC is deemed feasible if the outputs of the optimisation match the power losses and no network limits are exceeded (e.g., $\boldsymbol{PF} = 0$).

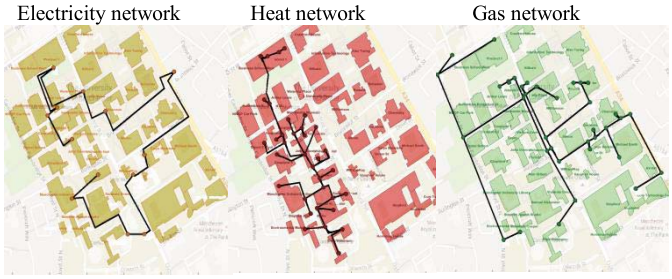

Fig. 3. Electricity, heat and gas networks.

IV. Case Study

Consider the real U.K. multi-energy district owned by The University of Manchester. The district comprises 26 buildings with a total annual demand of 28 GWhe (6 MWe peak) of electricity and 18 GWhth (12 MWth peak) of heat. Based on existing infrastructure and investment plans, it is assumed that 2.7 MWe, 2.6 MWth, 3.4 MWe and 24 MWth of CHP, EHP, PV and gas boiler capacity (i.e., 60 devices) are available in the district. These technologies allow multi-energy exchanges between buildings through the integrated 6.6kV (13 nodes) electricity network, 85°C (36 nodes) heat network, and 37 nodes gas network (see Fig. 3). The electricity network is operated as a ring and is currently N-1 secure, while the heat and gas networks are oversized. See [4] for more details. A maximum error of 0.0001 is taken as the termination criterion for the integrated network model and the two-stage approach. A lower error threshold could be used at the expense of increasing computational time.

For the purposes of this work, besides addressing the current conditions of the district, the study also aims at exploring different levels of network stress, uncertainty and penetration of EES and TES. Hence, day-ahead set points (with a half hourly resolution to match the U.K. market) are formulated using the proposed methodology. Focus will be put on impacts of network limits and use of storage, as well as on the computational efficiency. As there is no other model available that can be compared with the proposed framework, the energy and network results have been independently validated. For this purpose, decoupled network models were used to validate the network flows (i.e., independent network models from [4] and [9]). The district operation was assessed through simulations (i.e., the MILP constraints were simulated in MATLAB), whereas specific cases (e.g., deterministic and without network constraint violations) where validated with existing tools [28]. All studies were performed with an i7-4770 @3.40GHz processor and 16GB of RAM.

A. Deterministic Assessment

As a starting point, consider a January winter peak weekday. Under business-as-usual practices, most or all controllable devices within the district are operated to follow heat demand. Assuming an energy price spike caused by transmission charges (i.e., TRIAD mechanism in the U.K. [36]), and (1), the district would pay 25.3 k£ for energy that day. However, these costs could be reduced to 24.5 k£ (i.e., 3% saving) by

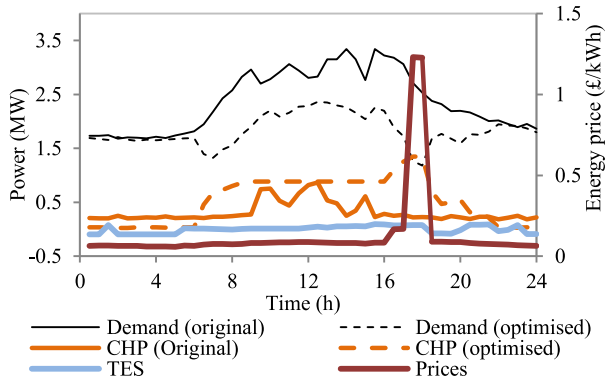

Fig. 4. Heat following and optimised dispatch considering dynamic prices.

TABLE I
DAILY ENERGY COSTS CONSIDERING DIFFERENT EES AND TES PENETRATION AND NETWORK CONSTRAINTS

Installed capacity		Network constraints (extreme case per network)		
EES	TES	Electricity	Heat	Gas
0	0	25.5 k£	26.9 k£	25.9 k£
1kW	1m^3	25.4 k£	26.8 k£	25.8 k£
10 kW	10 m^3	25.1 k£	26.3 k£	25.5 k£

optimising the operation of existing CHP and EHP units (see Fig. 4). Note that this is feasible as TRIAD warnings are issued one day in advance. As illustrated in the figure, similar savings could be achieved with storage (9 m^3 of TES is selected in the example to match the savings).

This smart district operation is based on the premise that the network can support multi-vector exchanges between the buildings. This is true in this particular case, as the networks are currently oversized. Thus, the two-stage approach is only used to address losses throughout the integrated networks, which does not have a noticeable impact on the operation of the district. Conversely, the operation of the district would have to be adjusted in the face of network stress conditions, as is further discussed below.

B. Network Stress Conditions

For the sake of comparison, rather than increasing energy demand, the firm (or N-1 secure) capacities of the electricity, heat and gas networks are artificially reduced to constrain the optimal operation of the district and thus demonstrate the model's ability to deal with network congestions. The energy costs (as denoted by (1)) associated with the specific day discussed above, and different levels of EES and TES penetration are presented in Table I. It is worth noting that the penetration levels were arbitrarily defined by adding 1kW (1m^3) or 10kW (10m^3) of EES (TES) capacity to each building. The network constraints were defined as extreme cases for each independent network where the district is still able to supply all customers (i.e., without curtailment).

As shown in the table, the added flexibility introduced by storage mitigates the costs introduced by network constraints. However, the results also demonstrate that different network constraints can cause significantly different costs.

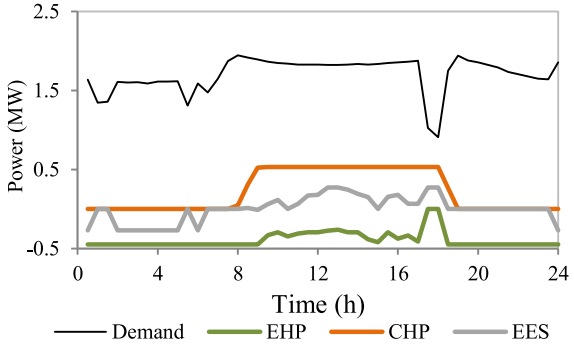

Fig. 5. Aggregated electricity flows considering network limits.

This is reasonable considering that, depending on the available technologies, districts will become less or more dependent on specific networks. For example, the optimal operation of the Manchester district relies on the effective use of CHP. This was shown in Fig. 4, where the CHP units were dispatched to minimise consumption during the high price period. The same trend can be seen in Fig. 5 where CHP is the main technology used to flatten demand in response to a constraint in the electricity network. As the effective use of CHP is based on the consumption of cogenerated heat within the district, constraints that limit the use of heat are particularly detrimental for this district (i.e., heat network constrains are the most costly in Table I).

It is important to emphasize that, under current network planning practices, the network is unlikely to face such extreme limitations as the one presented in Fig. 5. The reason being that network operator would normally reinforce the network before firm capacity is reached. Nevertheless, as discussed throughout this paper, it will become increasingly expensive to keep current reinforcement practices if large loads (e.g., electric vehicles) and smart districts and other prosumers emerge. In this context, there may be a business case for smart districts to provide network support through capacity services [1]. However, understanding and quantifying the value of such capacity services would require detailed economic and technical modelling of the networks (including planning) and smart districts. The proposed methodology can be used for the latter.

C. Stochastic Assessment

The results presented above are based on perfect information and may not represent realistic conditions where demand, renewable generation and other parameters may differ from their forecasted values. Accordingly, the study is extended to account for uncertainty based on the robust and flexibility constraints presented in Section III-B. Uncertainty is modelled as scenarios with variations (up to $\pm 10\%$) of electricity and heat demand as well as solar radiation. Two extreme conditions are used for the robust constraints, namely, highest demand and lowest solar radiation, and vice versa. Five or nine binomial scenario trees spanning from the average scenario every time period are used for the flexibility constraints. The expected energy costs under different levels of storage penetration are

TABLE II
ENERGY COSTS CONSIDERING DIFFERENT EES AND TES PENETRATION LEVELS AND NETWORK CONSTRAINTS

Installed capacity		Uncertainty cases (number of scenarios)				
EES	TES	Determi-nistic	Five		Nine	
			Cost	VPI	Cost	VPI
0	0	25.5 k£	28.2 k£	3.51 k£	28.2 k£	3.44 k£
1kW	1m^3	25.4 k£	27.8 k£	3.24 k£	27.8 k£	3.17 k£
10 kW	10 m^3	25.1 k£	25.4 k£	0.65 k£	25.1 k£	0.61 k£

TABLE III
COMPUTATIONAL TIME ASSESSMENT CONSIDERING DIFFERENT LEVELS OF UNCERTAINTY

Case	Model		
	LP	MILP	Full MILP
Deterministic	5.4 secs	9.5 secs	21 secs
Five scenarios	25.3 secs	78 secs	311 secs
Nine scenarios	84.44 secs	244 secs	840 secs

presented in Table II. In addition, as the expected costs do not capture the nature of uncertainty (e.g., the tendency of the scenarios to lead to lower or higher costs than in the deterministic scenario), the expected Value of Perfect Information (VPI) is also presented.

The results show that, as expected, energy costs increase for higher uncertainty levels. However, this effect can be mitigated with the additional flexibility introduced by storage, which effectively mitigates operational uncertainty. It can also be seen that the expected costs remain roughly the same after increasing the number of flexibility constraints from five to nine. Regardless, the expected VPI demonstrates that the additional flexibility constraints facilitate savings, particularly when little or no (flexible) storage is available. These results highlight that the flexibility constraints are adequate to represent uncertainty as envisioned in this study. However, in practice, forecasted uncertainty may be more complex and, thus, the selection of an adequate number of flexibility constraints would require dedicated studies, as the addition of flexibility constraints increases computational time, while gradually providing fewer benefits due to saturation.

D. Computational Costs and Scalability

Within the context of this study, the proposed model generally identified optimal solutions for deterministic and stochastic cases within 30 seconds and 500 seconds, respectively. This is clearly acceptable considering the half hourly resolution assumed in this work (based on the U.K. market). As the proposed framework is based on a MILP formulation, the main parameters that influence computational cost are the number of constraints and variables, particularly integer variables. The number of constraints and variables is dictated by the scenarios and devices considered. In this work, up to 398800 constraints and 246761 variables, including 31571 discrete variables, are required when modelling nine scenarios and all devices in every building. The network limits can also influence the speed of the model, as actively managing network violations with the two-stage approach would require additional iterations between the MILP and the integrated network models due to conflicting constraints across different networks. For example, while additional CHP generation might be called for alleviating congestions in the electricity network, at the same time, lower heat generation might be needed due to heat network limits.

An assessment of the computational performance of the algorithm subject to best, envisioned and worst conditions is presented in Table III. The LP study is meant to highlight conditions that facilitate formulating solutions quickly. This includes relaxing the optimisation model (removing all binary variables) and addressing networks with little or no constraints. The MILP study represents the typical applications envisioned for the proposed approach. That is the proposed MILP formulation of the model presented in Section III is used, and the model is applied to districts with significant penetration of storage, which are connected to constrained networks. The full MILP study is a worst case scenario assessment where each building includes Boilers, EES, TES, EHP and CHP. In addition, all units are modelled with integer variables.

The table shows that, even in the worst case conditions, the computational performance of the proposed model is adequate for the current case study. That is, the model can identify solutions within a reasonable time frame for districts with roughly 26 buildings, each with five controllable devices (130 devices), while considering constrained integrated networks and uncertainty.

Larger scale applications of the model may be achieved by aggregating resources, e.g., at the building or district levels. Afterwards, the different buildings/districts may exchange information, energy, cash and other vectors with the aim of improving their welfare and that of the overall community. However, proper transactive energy markets and mechanisms would practically be needed to enable very large scale (e.g., city level) applications [1]. Such approaches must recognise and incentivise energy from different aggregates, especially when provision of a specific system service comes to a specific cost.

V. CONCLUSION

This paper introduced a model for the operational optimisation of smart multi-energy districts subject to internal energy network constraints and considering relevant uncertainties. To be more specific, a two-stage robust, stochastic framework that combines MILP formulations with detailed nonlinear integrated network steady-state simulation models has been proposed for multi-temporal time-ahead energy management of smart multi-energy districts. Novel specific features also include multi-dimensional linked lists to improve computational efficiency of the stochastic model.

The model has been demonstrated with case studies based on a real multi-energy district, and a wide range of considerations for integrated network stress, uncertainty and storage levels. The results demonstrate that the physical limitations of the integrated network and uncertainty from demand and particular energy sources (e.g., PV) reduce the flexibility of the district. However, storage can be used as a source of multi-energy flexibility to manage and hedge against the impacts of network constraints and uncertainty.

Work in progress aims at extending the study to address several larger communities at, for example, the city level.

REFERENCES

[1] N. Good, E. A. M. Ceseña, and P. Mancarella, "Ten questions concerning smart districts," *Build. Environ.*, vol. 118, pp. 362–376, Jun. 2017.

[2] N. Good, E. A. M. Ceseña, L. Zhang, and P. Mancarella, "Techno-economic and business case assessment of low carbon technologies in distributed multi-energy systems," *Appl. Energy*, vol. 167, pp. 158–172, Apr. 2016.

[3] P. Mancarella, G. Andersson, J. A. Peças-Lopes, and K. R. W. Bell, "Modelling of integrated multi-energy systems: Drivers, requirements, and opportunities," in *Proc. Power Syst. Comput. Conf. (PSCC)*, Genoa, Italy, 2016, pp. 1–22.

[4] X. Liu and P. Mancarella, "Modelling, assessment and Sankey diagrams of integrated electricity-heat-gas networks in multi-vector district energy systems," *Appl. Energy*, vol. 167, pp. 336–352, Apr. 2016.

[5] M. C. Bozchalui, S. A. Hashmi, H. Hassen, C. A. Canizares, and K. Bhattacharya, "Optimal operation of residential energy hubs in smart grids," *IEEE Trans. Smart Grid*, vol. 3, no. 4, pp. 1755–1766, Dec. 2012.

[6] N. Li *et al.*, "Flexible operation of batteries in power system scheduling with renewable energy," *IEEE Trans. Sustain. Energy*, vol. 7, no. 2, pp. 685–696, Apr. 2016.

[7] N. Good and P. Mancarella, "Flexibility in multi-energy communities with electrical and thermal storage: A stochastic, robust optimization model for multi-service demand response," *IEEE Trans. Smart Grid*, to be published.

[8] M. Geidl and G. Andersson, "Optimal power flow of multiple energy carriers," *IEEE Trans. Power Syst.*, vol. 22, no. 1, pp. 145–155, Feb. 2007.

[9] X. Liu, J. Wu, N. Jenkins, and A. Bagdanavicius, "Combined analysis of electricity and heat networks," *Appl. Energy*, vol. 162, pp. 1238–1250, Jan. 2016.

[10] D. Zhang and D. Dechev, "A lock-free priority queue design based on multi-dimensional linked lists," *IEEE Trans. Parallel Distrib. Syst.*, vol. 27, no. 3, pp. 613–626, Mar. 2016.

[11] E. A. M. Ceseña, N. Good, A. L. A. Syrri, and P. Mancarella, "Techno-economic and business case assessment of multi-energy microgrids with co-optimization of energy, reserve and reliability services," *Appl. Energy*, vol. 210, pp. 896–913, Jan. 2018.

[12] M. Yazdani-Damavandi, N. Neyestani, M. Shafie-Khah, J. Contreras, and J. P. S. Catalão, "Strategic behavior of multi-energy players in electricity markets as aggregators of demand side resources using a Bi-level approach," *IEEE Trans. Power Syst.*, vol. 33, no. 1, pp. 397–411, Jan. 2018.

[13] H. Abdi, S. D. Beigvand, and M. La Scala, "A review of optimal power flow studies applied to smart grids and microgrids," *Renew. Sustain. Energy Rev.*, vol. 71, pp. 742–766, May 2017.

[14] Q. P. Zheng, J. Wang, and A. L. Liu, "Stochastic optimization for unit commitment—A review," *IEEE Trans. Power Syst.*, vol. 30, no. 4, pp. 1913–1924, Jul. 2015.

[15] R. A. Jabr, S. Karaki, and J. A. Korbane, "Robust multi-period OPF with storage and renewables," *IEEE Trans. Power Syst.*, vol. 30, no. 5, pp. 2790–2799, Sep. 2015.

[16] Y. Levron, J. M. Guerrero, and Y. Beck, "Optimal power flow in microgrids with energy storage," *IEEE Trans. Power Syst.*, vol. 28, no. 3, pp. 3226–3234, Aug. 2013.

[17] Á. Lorca and X. A. Sun, "Multistage robust unit commitment with dynamic uncertainty sets and energy storage," *IEEE Trans. Power Syst.*, vol. 32, no. 3, pp. 1678–1688, May 2017.

[18] M. Almassalkhi and I. Hiskens, "Optimization framework for the analysis of large-scale networks of energy hubs," in *Proc. 17th Power Syst. Comput. Conf. (PSCC)*, 2011, pp. 1–7.

[19] W. Huang, N. Zhang, J. Yang, Y. Wang, and C. Kang, "Optimal configuration planning of multi-energy systems considering distributed renewable energy," *IEEE Trans. Smart Grid*, to be published.

[20] B. Morvaj, R. Evins, and J. Carmeliet, "Optimization framework for distributed energy systems with integrated electrical grid constraints," *Appl. Energy*, vol. 171, pp. 296–313, Jun. 2016.

[21] W. Zhong, K. Xie, Y. Liu, C. Yang, and S. Xie, "Auction mechanisms for energy trading in multi-energy systems," *IEEE Trans. Ind. Informat.*, vol. 14, no. 4, pp. 1511–1521, Apr. 2018.

[22] S. Chen and C.-C. Liu, "From demand response to transactive energy: The state-of-the-art," *J. Mod. Power Syst. Clean Energy*, vol. 5, no. 1, pp. 10–19, 2017.

[23] S. Chen, Z. Wei, G. Sun, K. W. Cheung, and Y. Sun, "Multi-linear probabilistic energy flow analysis of integrated electrical and natural-gas systems," *IEEE Trans. Power Syst.*, vol. 32, no. 3, pp. 1970–1979, May 2017.

[24] S. Clegg and P. Mancarella, "Integrated electrical and gas network flexibility assessment in low-carbon multi-energy systems," *IEEE Trans. Sustain. Energy*, vol. 7, no. 2, pp. 718–731, Apr. 2016.

[25] S. Lei, J. Wang, C. Chen, and Y. Hou, "Mobile emergency generator pre-positioning and real-time allocation for resilient response to natural disasters," *IEEE Trans. Smart Grid*, vol. 9, no. 3, pp. 2030–2041, May 2018.

[26] S. Frank and S. Rebennack, "An introduction to optimal power flow: Theory, formulation, and examples," *IIE Trans.*, vol. 48, no. 12, pp. 1172–1197, Aug. 2016.

[27] R. Palma-Behnke, L. S. Vargas, J. R. Perez, J. D. Nunez, and R. A. Torres, "OPF With SVC and UPFC modeling for longitudinal systems," *IEEE Trans. Power Syst.*, vol. 19, no. 4, pp. 1742–1753, Nov. 2004.

[28] E. A. M. Ceseña, T. Capuder, and P. Mancarella, "Flexible distributed multienergy generation system expansion planning under uncertainty," *IEEE Trans. Smart Grid*, vol. 7, no. 1, pp. 348–357, Jan. 2016.

[29] C. Milan, M. Stadler, G. Cardoso, and S. Mashayekh, "Modeling of non-linear CHP efficiency curves in distributed energy systems," *Appl. Energy*, vol. 148, pp. 334–347, Jun. 2015.

[30] P. Fortenbacher and G. Andersson, "Battery degradation maps for power system optimization and as a benchmark reference," in *Proc. IEEE Manchester PowerTech*, Manchester, U.K., 2017, pp. 1–6.

[31] A. Kargarian, G. Hug, and J. Mohammadi, "A multi-time scale co-optimization method for sizing of energy storage and fast-ramping generation," *IEEE Trans. Sustain. Energy*, vol. 7, no. 4, pp. 1351–1361, Oct. 2016.

[32] R. E. Ciez and J. F. Whitacre, "Comparative techno-economic analysis of hybrid micro-grid systems utilizing different battery types," *Energy Convers. Manag.*, vol. 112, pp. 435–444, Mar. 2016.

[33] A. Boardman, S. Mockford, and P. Lawson, *Guidance for the Application of ENA ER P2/6 Security of Supply*, document EDS 08-0119, U.K., Power Netw., London, U.K., 2014.

[34] N. Amjady, S. Dehghan, A. Attarha, and A. J. Conejo, "Adaptive robust network-constrained AC unit commitment," *IEEE Trans. Power Syst.*, vol. 32, no. 1, pp. 672–683, Jan. 2017.

[35] L. Bai *et al.*, "Interval optimization based operating strategy for gas-electricity integrated energy systems considering demand response and wind uncertainty," *Appl. Energy*, vol. 167, pp. 270–279, Apr. 2016.

[36] National Grid. (2017). *Transmission Electricity Charges TNUoS Triad Data National Grid*. Accessed: Mar. 27, 2017. [Online]. Available:http://www2.nationalgrid.com/UK/Industry-information/System-charges/Electricity-transmission/Transmission-Network-Use-of-System-Charges/Transmission-Charges-Triad-Data/

Eduardo Alejandro Martínez Ceseña (S'06–M'13) received the M.Sc. degree in power systems from the Instituto Tecnológico de Morelia, Mexico, in 2008 and the Ph.D. degree in power systems from the University of Manchester, Manchester, U.K., in 2012.

He is currently a Research Associate with the Electrical Energy and Power Systems Group, University of Manchester. His research interests include the planning and design of electricity infrastructure under uncertainty (e.g., PV systems, wind farms, and distribution networks), power system economics, optimization techniques, and transactive operation of community multienergy systems in light of local and system level needs.

Pierluigi Mancarella (M'08–SM'14) received the M.Sc. and Ph.D. degrees in electrical energy systems from the Politecnico di Torino, Turin, Italy, in 2002 and 2006, respectively.

He is currently a Chair Professor of electrical power systems with the University of Melbourne, Australia, and a Professor of smart energy systems with the University of Manchester, U.K. His research interests include multienergy systems, power system integration of low carbon technologies, network planning under uncertainty, and risk and resilience of smart grids. He is an Editor of the IEEE TRANSACTIONS ON SMART GRID, an Associate Editor of the IEEE SYSTEMS JOURNAL, and an IEEE PES Distinguished Lecturer.